ChemComm

COMMUNICATION

View Article Online
View Journal | View Issue

Cite this: *Chem. Commun.*, 2024, **60**, 11794

Received 7th August 2024,
Accepted 28th August 2024

DOI: 10.1039/d4cc04017a

rsc.li/chemcomm

Plasmonic circular dichroism-based metal ion detection using gold nanorod–DNA complexes†

Yali Shi,‡[a] Satoshi Nakamura, ‡*[bc] Hideyuki Mitomo, [bd] Yusuke Yonamine,[b] Guoqing Wang [e] and Kuniharu Ijiro *[b]

We report that complexes formed between gold nanorods (AuNRs) and metal-mediated DNA exhibit plasmonic circular dichroism (CD) signals up to ~400 times stronger than the molecular CD signal of DNA. This substantial enhancement enables the detection of metal ions, offering a promising approach to analytical applications in chiral biochemistry.

DNA has several advantages that make it an excellent biosensing probe.[1–3] First, by designing the base sequence, DNA can recognize various target substances such as metal ions,[4] small molecules[5,6] and proteins.[7] Second, DNA can undergo conformational changes upon recognition of a target substance.[8] By taking advantage of these features, a variety of methods have been developed for the detection of target substances.[1–3] For example, the analyte-triggered oligodeoxynucleotide (ODN) conformational change can be converted into an optical or electrical signal by modification with fluorophores[9] or electroactive moieties.[10] Plasmonic nanoparticles, such as gold nanoparticles, are also a powerful tool for converting ODN conformational changes into an optical signal.[11] Due to localized surface plasmon resonance (LSPR), plasmonic nanoparticles exhibit a color change in accordance with the distance between the particles.[12] This color change can be triggered by probe ODNs on the particle surface for detection of target substances.[13] In addition, as DNA is a chiral molecule, its conformational changes can be directly detected with a circular dichroism (CD) spectrometer,[14] although CD spectroscopy suffers from low detection sensitivity. For example, for a 20-base pair double-stranded (ds)ODN, a high sample concentration of ~2 μM is required to obtain a CD signal.[14] Thus, CD spectroscopy has not been widely used for DNA-based biosensors.

Induced plasmonic chirality, a phenomenon in which an achiral plasmonic nanostructure becomes optically active in response to chiral molecules,[15,16] may help overcome this shortcoming. It is known that plasmonic CD is induced by dipole–dipole interactions between chiral adsorbates and plasmon nanostructures and/or by the chiral assembly of plasmonic nanoparticles.[16] One notable aspect of this phenomenon is that the intensity of the plasmonic CD is much higher than that of the molecular CD.[17–20] For example, Kneer *et al.* sandwiched a DNA origami sheet between two gold nanorods (AuNRs) and demonstrated the emergence of plasmonic CD signals ~300 times more intense than that of the DNA origami.[19] Chiral self-assemblies of AuNRs induced by helical polymers showed a strong CD response in the vis-NIR region.[21] Serum albumin and AuNR complexes provided strong plasmonic CD[16,22–24] and chiral assemblies of AuNRs as revealed by cryo-transmission electron microscopy (TEM).[16] However, the relationship between the protein structure and plasmonic CD of AuNR–protein complexes remains unclear due to the complex protein structures.[24] Based on our previous studies of plasmonic AuNR–DNA complexes,[25–28] DNA can be utilized as an ideal molecule for the construction of nanoparticle–molecule complexes to induce plasmonic CD, owing to the clearer structural information. By leveraging these attributes, not only are the potential applications of such complexes expanded in terms of chiral sensing, but it also paves the way for deeper explorations into chiroptical mechanisms in nanoparticle–molecule complexes.

Although the molecular structure required to induce plasmonic chirality remains controversial, a common feature of

[a] *Graduate School of Life Science, Hokkaido University, Kita 10, Nishi 8, Kita-Ku, Sapporo 060-0810, Japan*
[b] *Research Institute for Electronic Science, Hokkaido University, Kita 21, Nishi 10, Kita-ku, Sapporo, Hokkaido 001-0021, Japan. E-mail: ijiro@es.hokudai.ac.jp*
[c] *Institute for the Promotion of General Graduate Education (IPGE), Yamagata University, 4-3-16 Jonan, Yonezawa, Yamagata 992-8510, Japan. E-mail: s.nakamura@yz.yamagata-u.ac.jp*
[d] *Institute of Multidisciplinary Research for Advanced Materials, Tohoku University, Sendai, 980-8577, Japan*
[e] *MOE Key Laboratory of Evolution and Marine Biodiversity and Institute of Evolution and Marine Biodiversity, Ocean University of China, Qingdao 266003, China*

† Electronic supplementary information (ESI) available. See DOI: https://doi.org/10.1039/d4cc04017a

‡ These authors contributed equally.

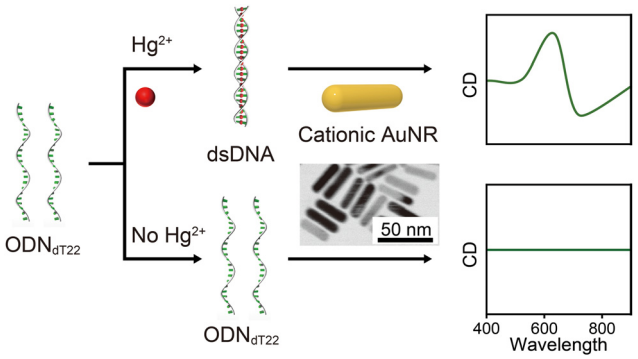

Scheme 1 Schematic illustration of this study. The AuNR–DNA complexes, showing plasmonic CD signals based on DNA conformational changes from random coil to helix, can be used for the detection of Hg^{2+}.

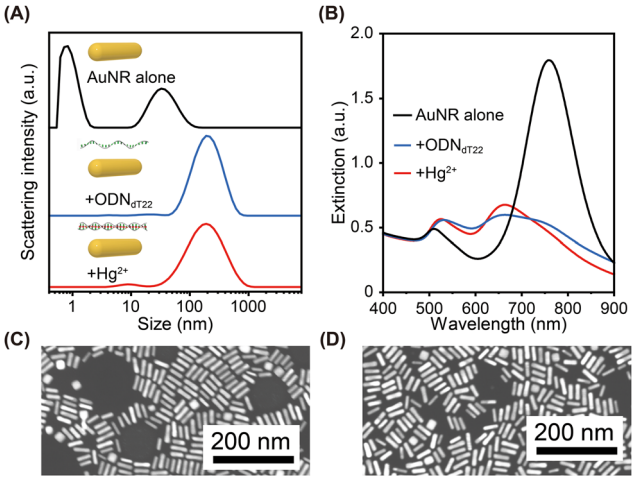

Fig. 1 (A) DLS profiles of AuNR alone (black line) and AuNR–ODN_{dT22} complexes prepared in the absence (blue line) or presence (red line) of Hg^{2+}. (B) Extinction spectra of AuNR alone (black line), and AuNR–ODN_{dT22} complexes prepared in the absence (blue line) or presence (red line) of Hg^{2+}. (C) and (D) Typical STEM images of the AuNR–ODN_{dT22} complexes prepared in the absence (C) and presence (D) of Hg^{2+}. (AuNRs: 16 nM; ODN_{dT22}: 0.6 μM; Hg^{2+}: 6.6 μM).

many of these molecules is a helical structure.[15–17,19,21–24,27,29,30] It is well known that Hg^{2+}, which is highly toxic to the human body, mediates thymine mismatching and forms thymine–Hg^{2+}–thymine (T–Hg^{II}–T) complexes.[31,32] Thus, single-stranded (ss)ODN can be hybridized to form dsDNA (helical structure) in the presence of Hg^{2+}. Additionally, thymine-rich ssDNA adopts a random coil structure (non-helical structure) due to weak base pair stacking interactions.[33] Based on this insight, in this study, we demonstrate that the plasmonic CD induced by AuNR–DNA complexes can be used for metal ion detection (Scheme 1).

First, we confirmed the structural changes in ODN_{dT22} (sequence: 5′-TTTTTTTTTTTTTTTTTTTTT-3′) through recognition of Hg^{2+}. We used Tris–HCl solutions for all experiments in this study. We measured the fluorescence intensity of a mixture of ODN_{dT22} (final concentration = 0.6 μM) and SYBR Green I (SG) containing Hg^{2+} and other metal ions (Ag^{+}, Cr^{6+}, Cu^{2+}, Fe^{3+}, and Zn^{2+}). Note that the concentration of metal ions was set to the minimum amount (6.6 μM) required for Hg^{2+} to mediate all of the thymine mismatches. SG stains dsDNA more efficiently than ssDNA;[34] therefore, by comparing fluorescence intensities, it is possible to confirm whether ODN_{dT22} adopts a ss or ds conformation. As expected, the fluorescence intensity of SG with Hg^{2+} was significantly greater than that for other metal ions or blank samples without Hg^{2+} (Fig. S1, ESI†). These results confirmed the ds formation of ODN_{dT22} by Hg^{2+} even under our experimental conditions.

Next, we investigated the formation of DNA complexes with AuNRs *via* electrostatic interactions. We prepared cationic AuNRs (size: ∼40 nm × ∼10 nm, zeta potential: +13.8 mV, final concentration = 16 nM) by the surface exchange of cetyltrimethylammonium bromide (CTAB)-covered AuNRs with primary amine-terminated hexaethylene glycol thiol ligands, to make them both more stable and controllable. Then, the cationic AuNRs were added into the Tris–HCl buffer solution containing ODN_{dT22} to form AuNR–DNA complexes. Dynamic light scattering (DLS) was used to characterize the complexes. As shown in Fig. 1A, AuNR alone showed DLS peaks at ∼1 nm and ∼39 nm. The former results from rotational motion and the latter results from translational motion.[35] The mixture of AuNRs and ODN_{dT22} showed a DLS peak at ∼150 nm, indicating complex formation. The position of this peak was almost completely independent of the Hg^{2+} concentration. We then measured the extinction spectra of AuNR alone and the AuNR–ODN_{dT22} complexes (Fig. 1B). AuNR alone showed a transverse (T)-LSPR peak at ∼510 nm and a longitudinal (L)-LSPR peak at ∼760 nm. In contrast, AuNR–ODN_{dT22} complexes exhibited a T-LSPR peak around ∼530 nm and a L-LSPR peak around ∼660 nm, regardless of the presence or absence of Hg^{2+}. The shift in the L-LSPR peak to a shorter wavelength indicates that the AuNRs assembled in a side-by-side manner.[36,37] This was also supported by scanning transmission electron microscopy (STEM) imaging (Fig. 1C and D). The above DLS and extinction spectra results demonstrated the successful formation of AuNR–DNA complexes.

Although the size and morphology of the AuNRs assemblies did not differ markedly (Fig. 1), there was a clear difference between the optical activities of the AuNR–ODN_{dT22} complexes with and without Hg^{2+}. Fig. 2A shows their CD spectra. Note that all CD spectra shown in this work have been smoothed using the Savitzky–Golay method (Fig. S2, ESI†).[38] In the absence of Hg^{2+}, neither AuNR alone nor the AuNR–ODN_{dT22} complexes showed plasmonic CD in the visible region (Fig. 2A). In contrast, the AuNR–ODN_{dT22} complexes with Hg^{2+} showed negative couplet CD with a dip at ∼720 nm and a peak at ∼620 nm. In the UV region, the AuNR–ODN_{dT22} complexes with Hg^{2+} exhibit similar but distinct CD characteristics to those without AuNRs in the same region due to the large electromagnetic field near the Hg^{2+}-mediated DNA.[39] Indeed, similar results were observed in the AuNR–dsDNA complexes in which dsDNA was formed by ODN_{dT22} and ODN_{dA22} (sequence: 5′-AAAAAAAAAAAAAAAAAAAAA-3′) (Fig. S3A, ESI†).

Here we emphasize three important characteristics. First, the plasmonic CD was much larger than the molecular CD of the DNA

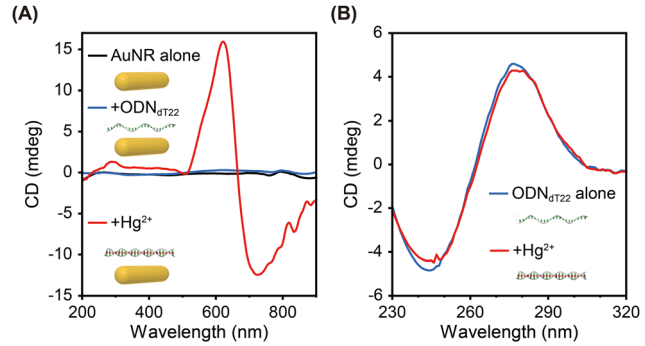

Fig. 2 CD spectra for (A) 16 nM AuNR alone (black line), AuNR and 0.6 μM ODN$_{dT22}$ complexes (blue line), AuNR and ODN$_{dT22}$ complexes with 6.6 μM Hg^{2+} (red line), (B) 20 μM ODN$_{dT22}$ alone (blue line) and with 220 μM Hg^{2+} (red line).

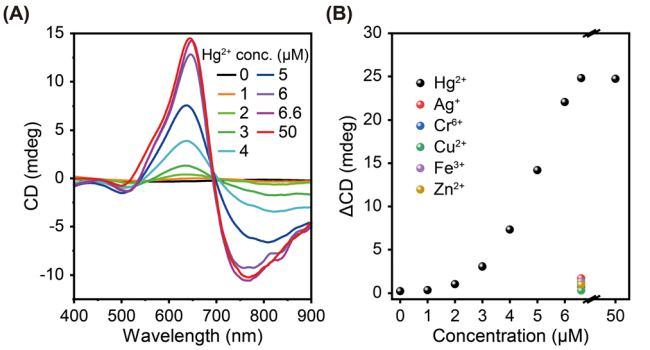

Fig. 3 (A) CD spectra for AuNR–ODN$_{dT22}$ complexes prepared at different concentrations of Hg^{2+}. (B) Plots of ΔCD *versus* Hg^{2+} or other metal ion concentrations (6.6 μM).

in the UV region (the plasmonic CD was detected even though the DNA was below the detection limit). To quantitatively compare the plasmonic CD with the CD of the DNA, we used the following equation:[17,20]

$$A_{CD} = \frac{\Delta CD_{(plasmon)}/c_{(DNA)}}{\Delta CD_{(DNA)}/c_{0(DNA)}}.$$

where A_{CD} is the enhancement factor, $\Delta CD_{(plasmon)}$ is the difference between the peak and dip values of the plasmonic CD signal, $c_{(DNA)}$ is the concentration of DNA in the AuNR–DNA complexes solution, $\Delta CD_{(DNA)}$ is the difference between the peak and dip values of the molecular CD signal of DNA alone, and $c_{0(DNA)}$ is the concentration of the DNA alone. As a result, the A_{CD} from AuNR–ODN$_{dT22}$ complexes at a Hg^{2+} concentration of 6.6 μM was calculated to be 97, indicating a significant advantage in terms of detection. Second, a clear change in plasmonic CD in the visible region was observed even with a low Hg^{2+} concentration (Fig. 2A), although the molecular CD of ODN$_{dT22}$ was almost unchanged with Hg^{2+} (Fig. 2B). However, dsDNA formation with ODN$_{dA22}$ caused a clear change in molecular CD (Fig. S3B, ESI†). Third, compared with SG fluoresce method (Fig. S1, ESI†), no strong background signal was observed in this system (Fig. 2A). These results suggest that the AuNR–DNA complexes not only enhance the CD signal intensity of DNA but also recognize conformational changes in metal-mediated DNA, as a plasmonic CD signal, with greater sensitivity; thereby demonstrating their potential applications in metal ion detection.

In order to test the analytical performance with regard to metal ion detection using the AuNR–DNA complexes, the plasmonic chiroptical activities of the AuNR–ODN$_{dT22}$ complexes were recorded upon addition of Hg^{2+} at different concentrations (Fig. 3A). Even when the Hg^{2+} concentration was changed, the zero-crossing (~670 nm) and peak (~610 nm) positions remained nearly identical. In addition, as shown in Fig. S4 (ESI†), the zero-crossing and the L-LSPR peak were well matched. Fig. 3B plots the $\Delta CD_{(plasmon)}$ *versus* Hg^{2+} concentration, which shows that the plasmonic CD began to be detected around the Hg^{2+} concentration of 2 μM. This is consistent with the Hg^{2+} concentration at which ODN$_{dT22}$ began to form double strands (Fig. S1B, ESI†). When the concentration of Hg^{2+} was over 6.6 μM, ΔCD reached its largest value (~25 mdeg). The saturation may be explained by the fact that ssODN$_{dT22}$ was completely consumed in the presence of 6.6 μM of Hg^{2+}. It is also worth noting that the plasmonic CD signal in our system did not decrease, as in the fluorescence method, in the presence of high Hg^{2+} concentrations (Fig. S1, ESI†), indicating its good stability with regard to Hg^{2+} detection. We also tested the plasmonic CD responses to the other potential interfering compounds, including Ag^{+}, Cr^{6+}, Cu^{2+}, Fe^{3+}, and Zn^{2+}, under the same reaction conditions. Interestingly, except for Hg^{2+} with reproducibility (Fig. S5, ESI†), no obvious plasmonic CD signal was obtained in the presence of the other interfering ions (6.6 μM) in the sensing systems, indicating good selectivity toward Hg^{2+} (Fig. 3B). These results indicated that the AuNR–DNA complex system shows high analytical performance with regard to metal ions.

The advantage of our detection method is that the ion of interest can be changed simply by changing the base sequence. To demonstrate this, we performed an experiment using Ag^{+} as another model ion. For this experiment, a probe ODN with the sequence 5′-CCCCCCCCCCCCCCCCCCCCC-3′ (ODN$_{dC22}$) was used (Fig. 4A). ODN$_{dC22}$ underwent a conformation change caused by Ag^{+} as Ag^{+} mediates cytosine mismatching and formed cytosine–Ag^{+}–cytosine (C–Ag^{I}–C) base pairs,[40] as confirmed by CD measurements (Fig. 4B). As shown in Fig. 4A, the AuNR–ODN$_{dC22}$ complexes showed no plasmonic CD in the absence of Ag^{+}. However, in the presence of Ag^{+}, the AuNR–ODN$_{dC22}$ complexes exhibit negative couplet plasmonic CD. The A_{CD} from AuNR–ODN$_{dC22}$ complexes at Ag^{+} concentration of 6.6 μM was calculated to be 400. It is noteworthy that the AuNR–ODN$_{dC22}$ complexes exhibit a marked plasmonic CD. Specifically, AuNR–ODN$_{dC22}$ complexes with Ag^{+} (6.6 μM) show a higher value of *g*-factor (1.0×10^{-2}), which represents the dissymmetry, whereas the AuNR–ODN$_{dT22}$ complex with Hg^{2+} (6.6 μM) shows a lower value (0.09×10^{-2}) (Fig. S6) (details are in the ESI†). This value is comparable to that of the AuNR–protein complex system, which has side-by-side AuNR chiral assemblies (1.9×10^{-2}).[23]

In summary, we have demonstrated that conformational changes in DNA can be observed by the induced plasmonic optical

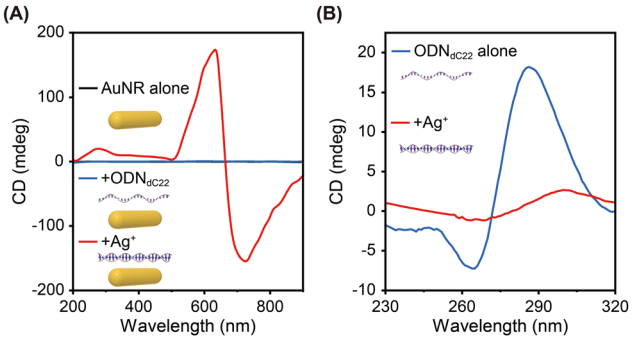

Fig. 4 CD spectra for (A) 16 nM AuNR alone (black line), AuNR and 0.6 μM ODN_{dC22} complexes (blue line), AuNR and ODN_{dC22} complexes with 6.6 μM Ag^+ (red line), (B) 20 μM ODN_{dC22} alone (blue line) and with 220 μM Ag^+ (red line).

activity from AuNR–DNA complexes, which has afforded the ability to detect metal ions (Hg^{2+} and Ag^+) with no significant background signal. Importantly, the induced plasmonic CD in the visible region was much larger than the molecular CD of the ODN in the UV region. It is also noteworthy that clear changes in plasmonic CD could be caused even with metal-mediated ODNs that show little molecular CD change. We believe that this study will inspire further research on chiral plasmonic applications and facilitate exploration into the chiroptical mechanisms.

We acknowledge financial support from the Japan Society for the Promotion of Science (JSPS) KAKENHI (Grant no. 24K03258 and 24K17574). S. N. acknowledges financial support from Iketani Science and Technology Foundation. K. I. acknowledges support from the "Photoexcitonix Project" and the "Project of Young Investigator Promotion" at Hokkaido University. This work was also supported in part by the Crossover Alliance to Create the Future with People, Intelligence and Materials" from the Ministry of Education, Culture, Sports, Science, and Technology of Japan (MEXT). A part of this work was supported by "Advanced Research Infrastructure for Materials and Nanotechnology in Japan (ARIM)" of the Ministry of Education, Culture, Sports, Science and Technology (MEXT): Grant Number JPMXP1223HK0051 and JPMXP1224HK0048 (Hokkaido University).

Data availability

The data supporting this article have been included as part of the ESI.†

Conflicts of interest

There are no conflicts to declare.

Notes and references

1 V. Tjong, L. Tang, S. Zauscher and A. Chilkoti, *Chem. Soc. Rev.*, 2014, **43**, 1612–1626.
2 H.-M. Meng, H. Liu, H. Kuai, R. Peng, L. Mo and X.-B. Zhang, *Chem. Soc. Rev.*, 2016, **45**, 2583–2602.
3 H. Yoo, H. Jo and S. S. Oh, *Mater. Adv.*, 2020, **1**, 2663–2687.
4 M. Rajendran and A. D. Ellington, *Anal. Bioanal. Chem.*, 2008, **390**, 1067–1075.
5 A. D. Ellington and J. W. Szostak, *Nature*, 1992, **355**, 850–852.
6 D. E. Huizenga and J. W. Szostak, *Biochemistry*, 1995, **34**, 656–665.
7 L. C. Bock, L. C. Griffin, J. A. Latham, E. H. Vermaas and J. J. Toole, *Nature*, 1992, **355**, 564–566.
8 R. Nutiu and Y. Li, *Angew. Chem., Int. Ed.*, 2005, **44**, 1061–1065.
9 S. Tyagi and F. R. Kramer, *Nat. Biotechnol.*, 1996, **14**, 303–308.
10 C. Fan, K. W. Plaxco and A. J. Heeger, *Proc. Natl. Acad. Sci. U. S. A.*, 2003, **100**, 9134–9137.
11 K. Saha, S. S. Agasti, C. Kim, X. Li and V. M. Rotello, *Chem. Rev.*, 2012, **112**, 2739–2779.
12 S. K. Ghosh and T. Pal, *Chem. Rev.*, 2007, **107**, 4797–4862.
13 L. Wang, Z. He, Q. Chen, G. Wang, X. Liang, T. Takarada and M. Maeda, *ACS Sustainable Chem. Eng.*, 2023, **11**, 3611–3620.
14 J. Kypr, I. Kejnovská, D. Renčiuk and M. Vorlíčková, *Nucleic Acids Res.*, 2009, **37**, 1713–1725.
15 B. M. Maoz, Y. Chaikin, A. B. Tesler, O. B. Elli, Z. Fan, A. O. Govorov and G. Markovich, *Nano Lett.*, 2013, **13**, 1203–1209.
16 Q. Zhang, T. Hernandez, K. W. Smith, S. A. H. Jebeli, A. X. Dai, L. Warning, R. Baiyasi, L. A. McCarthy, H. Guo, D.-H. Chen, J. A. Dionne, C. F. Landes and S. Link, *Science*, 2019, **365**, 1475–1478.
17 F. Lu, Y. Tian, M. Liu, D. Su, H. Zhang, A. O. Govorov and O. Gang, *Nano Lett.*, 2013, **13**, 3145–3151.
18 R.-Y. Wang, P. Wang, Y. Liu, W. Zhao, D. Zhai, X. Hong, Y. Ji, X. Wu, F. Wang, D. Zhang, W. Zhang, R. Liu and X. Zhang, *J. Phys. Chem. C*, 2014, **118**, 9690–9695.
19 L. M. Kneer, E.-M. Roller, L. V. Besteiro, R. Schreiber, A. O. Govorov and T. Liedl, *ACS Nano*, 2018, **12**, 9110–9115.
20 W. Wang, F. Wu, Y. Zhang, W. Wei, W. Niu and G. Xu, *Chem. Commun.*, 2021, **57**, 7390–7393.
21 G. Cheng, D. Xu, Z. Lu and K. Liu, *ACS Nano*, 2019, **13**, 1479–1489.
22 S. Hou, H. Zhang, J. Yan, Y. Ji, T. Wen, W. Liu, Z. Hu and X. Wu, *Phys. Chem. Chem. Phys.*, 2015, **17**, 8187–8193.
23 H. Shinmori and C. Mochizuki, *Chem. Commun.*, 2017, **53**, 6569–6572.
24 L. A. Warning, A. R. Miandashti, A. Misiura, C. F. Landes and S. Link, *J. Phys. Chem. C*, 2022, **126**, 2656–2668.
25 S. Nakamura, H. Mitomo, M. Aizawa, T. Tani, Y. Matsuo, K. Niikura, A. Pike, M. Naya, A. Shishido and K. Ijiro, *ACS Omega*, 2017, **2**, 2208–2213.
26 S. Nakamura, H. Mitomo, Y. Sekizawa, T. Higuchi, Y. Matsuo, H. Jinnai and K. Ijiro, *Langmuir*, 2020, **36**, 3590–3599.
27 S. Nakamura, H. Mitomo, Y. Yonamine and K. Ijiro, *Chem. Lett.*, 2020, **49**, 749–752.
28 S. Nakamura, H. Mitomo, S. Suzuki, Y. Torii, Y. Sekizawa, Y. Yonamine and K. Ijiro, *Chem. Lett.*, 2022, **51**, 529–532.
29 Y. Zhu, L. Xu, W. Ma, Z. Xu, H. Kuang, L. Wang and C. Xu, *Chem. Commun.*, 2012, **48**, 11889–11891.
30 W. Ma, H. Kuang, L. Xu, L. Ding, C. Xu, L. Wang and N. A. Kotov, *Nat. Commun.*, 2013, **4**, 2689.
31 Y. Miyake, H. Togashi, M. Tashiro, H. Yamaguchi, S. Oda, M. Kudo, Y. Tanaka, Y. Kondo, R. Sawa, T. Fujimoto, T. Machinami and A. Ono, *J. Am. Chem. Soc.*, 2006, **128**, 2172–2173.
32 L. Benda, M. Straka, V. Sychrovský, P. Bouř and Y. Tanaka, *J. Phys. Chem. A*, 2012, **116**, 8313–8320.
33 W. Saenger, *Principles of Nucleic Acid Structure*, Springer New York, New York, NY, 1984.
34 H. Zipper, H. Brunner, J. Bernhagen and F. Vitzthum, *Nucleic Acids Res.*, 2004, **32**, e103.
35 M. Glidden and M. Muschol, *J. Phys. Chem. C*, 2012, **116**, 8128–8137.
36 M. Gluodenis and C. A. Foss, *J. Phys. Chem. B*, 2002, **106**, 9484–9489.
37 J. Yang, Y. Sekizawa, X. Shi, K. Ijiro and H. Mitomo, *Bull. Chem. Soc. Jpn.*, 2024, **97**, uoae073.
38 A. Savitzky and M. J. E. Golay, *Anal. Chem.*, 1964, **36**, 1627–1639.
39 Z. Zhu, W. Liu, Z. Li, B. Han, Y. Zhou, Y. Gao and Z. Tang, *ACS Nano*, 2012, **6**, 2326–2332.
40 A. Ono, S. Cao, H. Togashi, M. Tashiro, T. Fujimoto, T. Machinami, S. Oda, Y. Miyake, I. Okamoto and Y. Tanaka, *Chem. Commun.*, 2008, 4825–4827.